

WL-TR-97-3051

**Verification and Baseline Fatigue
Crack Growth Data of Ti-6-4,
430-195ksi Steel, and 7075-T73**



**J.H. Elsner, K.L. Boyd, S. Krishnan
Analytical Services and Materials, Inc.
107 Research Drive
Hampton, Virginia 23666**

**J.A. Harter
WL/FIBE, Bldg 65
2790 D Street, Rm 504
Wright-Patterson AFB, Ohio 45433-7402**

MARCH 1997

FINAL REPORT FOR 01 JAN - 30 SEP 1995

Approved for public release; distribution unlimited

19980225 082

DTIC QUALITY INSPECTED 4

**FLIGHT DYNAMICS DIRECTORATE
WRIGHT LABORATORY
AIR FORCE MATERIEL COMMAND
WRIGHT-PATTERSON AIR FORCE BASE, OH 45433-7562**

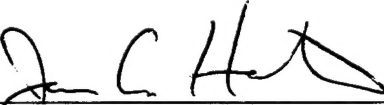
NOTICE

USING GOVERNMENT DRAWINGS, SPECIFICATIONS, OR OTHER DATA INCLUDED IN THIS DOCUMENT FOR ANY PURPOSE OTHER THAN GOVERNMENT PROCUREMENT DOES NOT IN ANY WAY OBLIGATE THE US GOVERNMENT. THE FACT THAT THE GOVERNMENT FORMULATED OR SUPPLIED THE DRAWINGS, SPECIFICATIONS, OR OTHER DATA DOES NOT LICENSE THE HOLDER OR ANY OTHER PERSON OR CORPORATION; OR CONVEY ANY RIGHTS OR PERMISSION TO MANUFACTURE, USE, OR SELL ANY PATENTED INVENTION THAT MAY RELATE TO THEM.

THIS REPORT IS RELEASABLE TO THE NATIONAL TECHNICAL INFORMATION SERVICE (NTIS). AT NTIS, IT WILL BE AVAILABLE TO THE GENERAL PUBLIC, INCLUDING FOREIGN NATIONS.

THIS TECHNICAL REPORT HAS BEEN REVIEWED AND IS APPROVED FOR PUBLICATION.


JOHN S. BROOKS
TEAM LEADER
STRUCTURAL INTEGRITY BRANCH


JAMES A. HARTER
AEROSPACE ENGINEER
STRUCTURAL INTEGRITY BRANCH


JOHN T. ACH
BRANCH CHIEF
STRUCTURAL INTEGRITY BRANCH

IF YOUR ADDRESS HAS CHANGED, IF YOU WISH TO BE REMOVED FROM OUR MAILING LIST, OR IF THE ADDRESSEE IS NO LONGER EMPLOYED BY YOUR ORGANIZATION, PLEASE NOTIFY WL/FIBE, BLDG 65, 2790 D ST., ROOM 504, WRIGHT-PATTERSON AFB OH 45433-7402 TO HELP MAINTAIN A CURRENT MAILING LIST.

Do not return copies of this report unless contractual obligations or notice on a specific document requires its return.

REPORT DOCUMENTATION PAGE			Form Approved OMB No. 0704-0188
<p>Public reporting burden for this collection of information is estimated to average 1 hour per response, including the time for reviewing instructions, searching existing data sources, gathering and maintaining the data needed, and completing and reviewing the collection of information. Send comments regarding this burden estimate or any other aspect of this collection of information, including suggestions for reducing this burden, to Washington Headquarters Services, Directorate for Information Operations and Reports, 1215 Jefferson Davis Highway, Suite 1204, Arlington, VA 22202-4302, and to the Office of Management and Budget, Paperwork Reduction Project (0704-0188), Washington, DC 20503.</p>			
1. AGENCY USE ONLY (Leave blank)	2. REPORT DATE	3. REPORT TYPE AND DATES COVERED	
	March 1997	FINAL	01/01/95 -- 09/30/95
4. TITLE AND SUBTITLE		5. FUNDING NUMBERS	
VERIFICATION AND BASELINE FATIGUE CRACK GROWTH DATA OF Ti-6-4, 4340-195ksi STEEL, AND 7075-T73		C: F33615-94-D-3212 PE: 62201 PR: 2401 TA: LE WU: 00	
6. AUTHOR(S) J.H. ELSNER, K.L. BOYD, S. KRISHNAN ANALYTICAL SERVICES & MATERIALS INC.		7. PERFORMING ORGANIZATION NAME(S) AND ADDRESS(ES) Analytical Services and Materials, Inc 107 Research Drive Hampton VA 23666	
		Structural Integrity Branch 2790 D Street, Room 504 WPAFB OH 45433-7402	
8. PERFORMING ORGANIZATION REPORT NUMBER		9. SPONSORING/MONITORING AGENCY NAME(S) AND ADDRESS(ES) FLIGHT DYNAMICS DIRECTORATE WRIGHT LABORATORY AIR FORCE MATERIEL COMMAND WRIGHT-PATTERSON AFB OH 45433-7562 POC: LT DAVID CONLEY, WL-FIBE, 937-255-3144	
10. SPONSORING/MONITORING AGENCY REPORT NUMBER WL-TR-97-3051		11. SUPPLEMENTARY NOTES	
12a. DISTRIBUTION AVAILABILITY STATEMENT APPROVED FOR PUBLIC RELEASE; DISTRIBUTION UNLIMITED		12b. DISTRIBUTION CODE	
13. ABSTRACT (Maximum 200 words)			
<p>This research included baseline crack growth data for Ti-6-4 and 4340-195ksi steel, verification testing of the Ti-6-4 data, testing various geometries, and AFGROW development Baseline test data were produced for Ti-6-4 and 4340-195ksi. Center crack specimens were tested at four stress ratios. Load shedding enabled crack growth rates as low as 10.0^{-9} to be recorded for both materials. Determining crack growth rates at this level is important for life predictions, since much of the life is accounted for when cracks are small. Open hole Ti-6-4 specimens were tested to verify the crack growth rate data generated and to test AFGROW's predictive abilities. For the six open hole specimens, AFGROW had an average error of 12%. Joint specimen also tested in order to verify AFGROW's abilities. These specimens were modeled with finite element analysis to determine the load transfer around the rivet holes. Once this was accomplished, predictions were run and compared to test data. The results of the single, multiple in-line joint, and multiple staggered joint specimens were good.</p>			
14. SUBJECT TERMS		15. NUMBER OF PAGES 34	
		16. PRICE CODE	
17. SECURITY CLASSIFICATION OF REPORT UNCLASSIFIED	18. SECURITY CLASSIFICATION OF THIS PAGE UNCLASSIFIED	19. SECURITY CLASSIFICATION OF ABSTRACT UNCLASSIFIED	20. LIMITATION OF ABSTRACT SAR

TABLE OF CONTENTS

LIST OF FIGURES	iv
LIST OF TABLES.....	vi
FOREWORD	vii
1. EXECUTIVE SUMMARY	1
2. INTRODUCTION	2
3. FINITE ELEMENT ANALYSIS	3
4. VERIFICATION TESTING.....	9
4.1. Center Cracked Panel Testing.....	9
4.1.1. Ti-6-4 Center Cracked Panel Testing.....	10
4.1.2. 4340-195ksi Steel Center Cracked Panel Testing.....	13
4.2. Open Hole Ti-6-4 Panel Testing	17
4.3. Fastener Joint Specimens.....	22
5. AFGROW ENHANCEMENTS.....	25
6. REFERENCES	29
7. APPENDIX.....	29
7.1 Detailed Specimen Information	29

LIST OF FIGURES

Figure 1: Bolted-Joint Configurations	3
Figure 2: Symmetry Planes Assumed for 2D Finite Element Analysis.....	4
Figure 3: Single Fastener Specimen	5
Figure 4: Area Modeled Using FRANC2D/L.....	7
Figure 5: Strip Model of Multi Fastener, In-Line Specimen	8
Figure 6: Crack Growth Rate Plot of Ti-6-4 Center Cracked Panels Using the Decreasing K Method with R=-0.5	10
Figure 7: Crack Growth Rate Plot of Ti-6-4 Center Cracked Panels Using the Decreasing K Method with R=-0.1.....	11
Figure 8: Crack Growth Rate Plot of Ti-6-4 Center Cracked Panels Using the Decreasing K Method with R=0.1.....	11
Figure 9: Crack Growth Rate Plot of Ti-6-4 Center Cracked Panels Using the Decreasing K Method with R=0.5.....	12
Figure 10: Composite of All Ti-6-4 Center Cracked Panel Tests. Each Series of R-ratio Data Represent Two Specimens.....	13
Figure 11: Crack Growth Rate Plot of 4340-195ksi Steel Center Cracked Panels Using the Decreasing K Method with R=-0.5.....	14
Figure 12: Crack Growth Rate Plot of 4340-195ksi Steel Center Cracked Panels Using the Decreasing K Method with R=-0.1.....	14
Figure 13: Crack Growth Rate Plot of 4340-195ksi Steel Center Cracked Panels Using the Decreasing K Method with R=0.1.....	15
Figure 14: Crack Growth Rate Plot of 4340-195ksi steel Center Cracked Panels Using the Decreasing K Method with R=0.5.....	15
Figure 15: Composite of All 4340-195ksi Steel Center Cracked Panel Tests. Each Series of R-ratio Data Represents Two Specimens.....	16
Figure 16: Same Graph as Figure 15 with Unreasonable Data Removed.	17

Figure 17: Test Data Shown in Figure 8 Plotted with AFGROW Database Plot for Various R-ratios	18
Figure 18: Constant Amplitude (16 kips) Testing Data of Ti-OH-1 and AFGROW Prediction.....	19
Figure 19: Constant Amplitude (16 kips) Testing Data of Ti-OH-2 and AFGROW Prediction.....	19
Figure 20: Constant Amplitude (18 kips) Testing Data of Ti-OH-3 and AFGROW Prediction.....	20
Figure 21: Constant Amplitude (18kips) Testing Data of Ti-OH-4 and AFGROW Prediction.....	20
Figure 22: Constant Amplitude (20 kips) Testing Data of Ti-OH-5 and AFGROW Prediction.....	21
Figure 23: Constant Amplitude (20 kips) Testing Data of Ti-OH-6 and AFGROW Prediction.....	21
Figure 24: Schematic of the Joint Specimens After Precracking but Before Riveting....	22
Figure 25: Schematic of Staggered Joint Specimen and Loads Used to Calculate Load Transfer Coefficient.....	23
Figure 26: Environment Dialog Box.....	25
Figure 27: Model With Two Environments Applied.....	26
Figure 28: Beta Factor Table.	27
Figure 29: Plot Window Showing Crack Length Versus Cycles.....	28

LIST OF TABLES

Table 1: Test Matrix.....	9
Table 2: Crack Sizes Input to AFGROW for Life Prediction Shown in Figures 17 - 22.	18
Table 3: Flawed Riveted Specimen Lifetimes and Information Used for AFGROW Predictions Where c is Measured and a is Calculated.	24

FOREWORD

This report was prepared by Analytical Services & Materials, Inc., Hampton Virginia for WL/FIBEC, Wright-Patterson Air Force Base, Ohio under contract F33615-94-D-3212, "Structural Integrity Analysis and Verification for Aircraft Structures." The contract program manager was 1st Lt Dave Conley, WL/FIBE. The government project engineer was James A. Harter. The period of performance for this report was 1 Jan 95 through 30 Sept 95.

The work was performed under project (Delivery Order 0003), by Analytical Services & Materials, Inc. personnel located at the WL/FIBEC Fatigue & Fracture Test Facility, Bldg. 65, Area B, Wright-Patterson AFB, OH. This effort was a follow up to previous work performed under Delivery Order 0001 [1]. The Principal Investigator of this research was Mr. Kevin L. Boyd. The authors of this report were Mr. John H. Elsner, Mr. Kevin L. Boyd, and Mr. Srinivas Krishnan. Technical inputs were submitted by Mr. James A. Harter and Mr. Daniel A. Jansen.

1. EXECUTIVE SUMMARY

This research included baseline crack growth data for Ti-6-4 and 4340-195ksi steel, verification testing of the Ti-6-4 data, testing various geometries, and AFGROW development.

Baseline test data were produced for Ti-6-4 and 4340-195ksi. Center cracked specimens were tested at four stress ratios. Load shedding enabled crack growth rates as low as 10.0^{-9} to be recorded for both materials. Determining crack growth rates at this level is important for life predictions since much of the life is accounted for when cracks are small.

Open hole Ti-6-4 specimens were tested to verify the crack growth rate data generated and to test AFGROW's predictive abilities. For the six open hole specimens, AFGROW had an average error of 12%.

Joint specimens were also tested in order to verify AFGROW's abilities. These specimens were modeled with finite element analysis to determine the load transfer around the rivet holes. Once this was accomplished, predictions were run and compared to test data. The results of the single, multiple in-line joint, and multiple staggered joint specimens were good.

2. INTRODUCTION

The purpose of this research is to determine fatigue crack growth rates for Ti-6-4 and 4340-195ksi steel and also to verify existing crack growth databases in AFGROW [2] by testing various geometries and comparing the predictions to test results. AFGROW is a fatigue crack growth prediction code developed by AS&M and the Air Force. In order to make AFGROW more useful, common structural materials need to be included in the material database that is included with the program. The materials database in AFGROW is based on simple middle tension (MT) or compact tension (CT) specimens. The majority of data are generated with MT specimens where data are sampled for as wide of a range of crack growth rate (da/dN) as possible. Normally, data in the range of 2.0 E-09 to 1.0 E-03 in/cycle are sampled using a decreasing – increasing delta K method. Of course, great care is taken to avoid overload effects as far as possible and data taken when delta K is increasing are compared to that taken during the initial decreasing period. The predictions, which rely on AFGROW's database, are then verified with test data that were generated with different and more complicated geometries.

3. FINITE ELEMENT ANALYSIS

The three bolted-joint configurations examined in this report were analyzed to estimate the amount of load transfer present in the specimens. This information was required so that the life predictions could be made for the bolted-joint configurations using the AFGROW crack growth life prediction code [2].

For this study, typical double shear joint specimens were designed to address an additional order of complexity in the life prediction process, or cracks growing from loaded holes. These “typical” joint configurations were designed with acceptable, industry-standard joint design parameters such as fastener size (0.25 in. typ.), pitch distance (1.0 in. typ.) and edge distances (0.75 in. typ.). The single fastener test specimens were 16.0 inches in length and 1.0 inch in width. The plate thicknesses for the single fastener specimens were 0.25 inch. The multiple fastener, in-line and staggered specimens were 16.0 inches in length and 3.95 inches in width. The plate thicknesses for the multiple fastener specimens were 0.09 inch. These specimen configurations and their crack locations can be seen below in Figure 1.

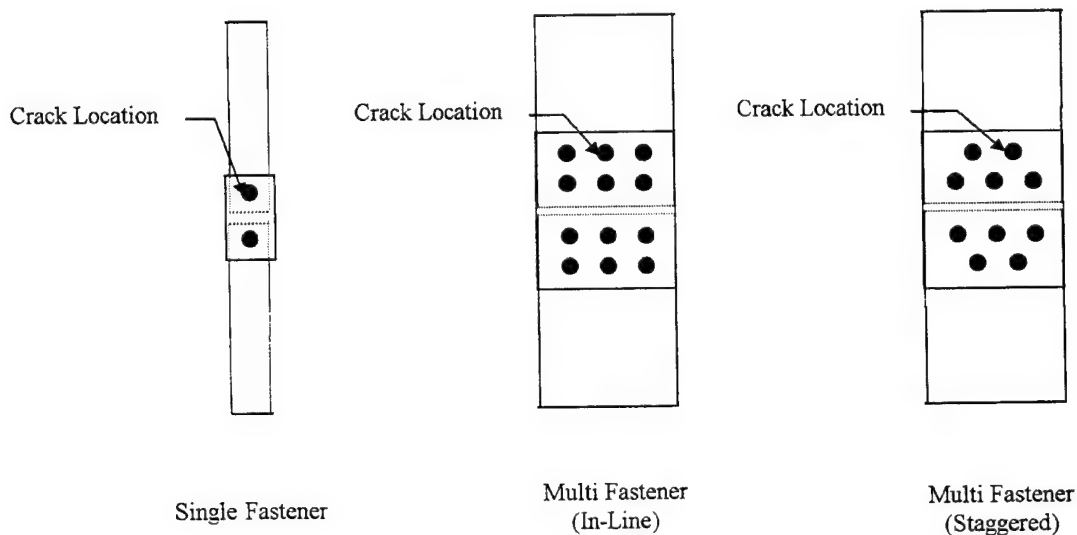


Figure 1: Bolted-Joint Configurations

All of the joint configurations modeled in this study were of the symmetric lap splice, or double shear configuration. These configurations were chosen to reduce the amount of bending present in the specimens during testing. During the testing phase of this study, all specimens were fatigued under uniaxial loading conditions. Also, all fasteners were protruding head, small clearance, or “neat” fit A286 steel fasteners that were lightly finger tightened, to remove the effect of load transfer through friction or “clamp-up” and/or pre-stress effects of the bolts.

The single fastener joint was assumed to have 100% load transfer for crack growth life prediction purposes. This joint configuration was verified with that FRANC2D/L finite element code [3] and is shown in Figure 3. Symmetry conditions were assumed both through the thickness of the joint and along the specimen’s length. The planes of symmetry assumed in the analysis can be seen below in Figure 2.

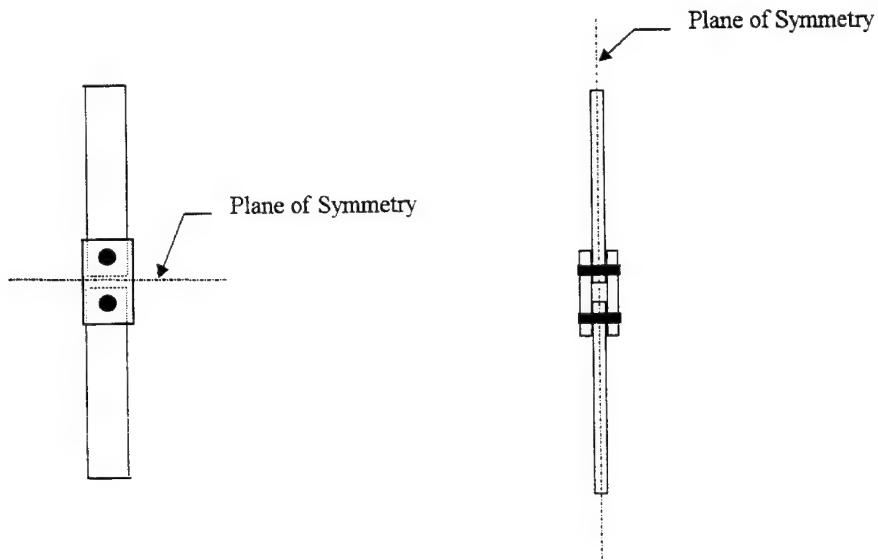


Figure 2: Symmetry Planes Assumed for 2D Finite Element Analysis

Because FRANC2D/L is a two dimensional layered code only one layer’s mesh can be seen at a time. The mesh for the “joined” member is shown in Figure 3. The “outlined” splice plates mesh must exactly mirror the mesh that is displayed within the confines of the displayed box. The mesh of the splice plate is not shown due to the redundancy of the mesh. The material properties used in the analysis are also shown in Figure 3. A unit remote load was applied to the specimen and the rivet load was calculated to be one (1.0), signifying 100% load transfer.

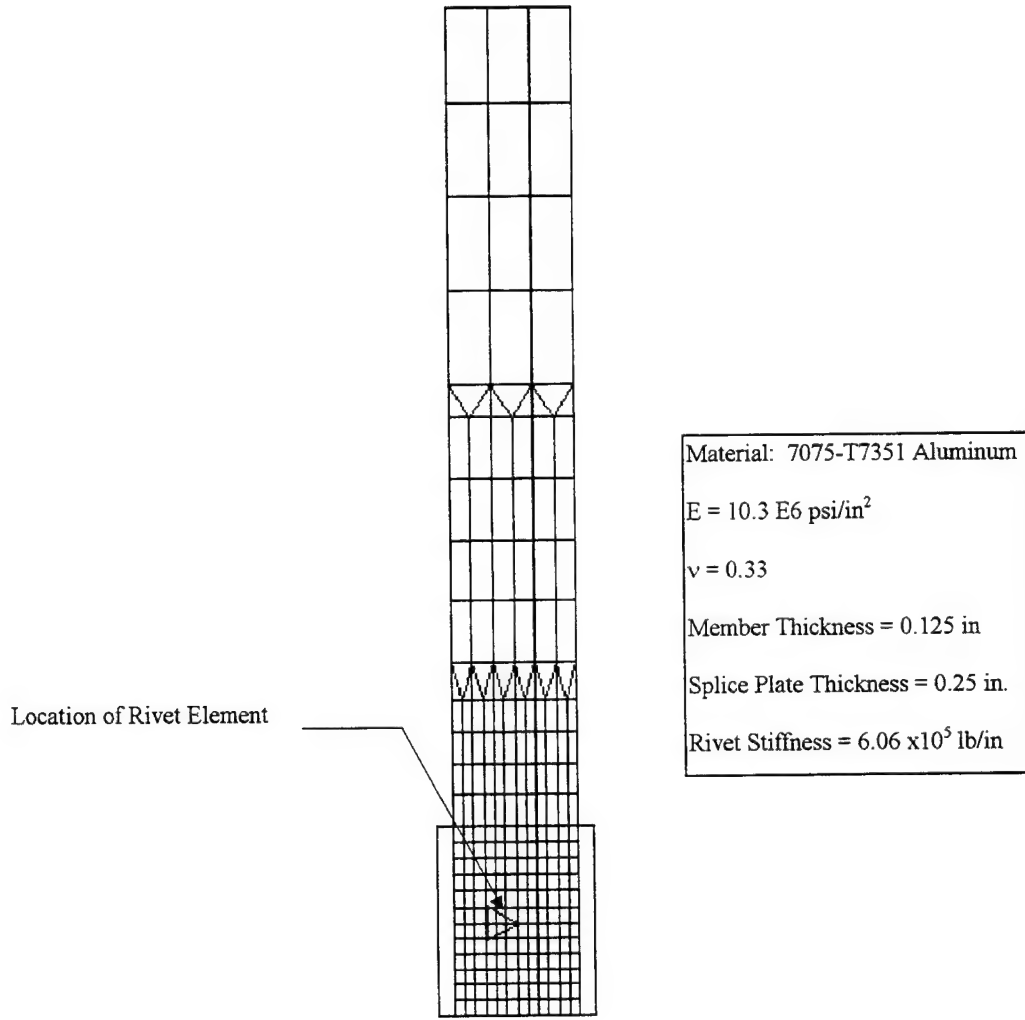


Figure 3: Single Fastener Specimen

The rivet's stiffness was calculated using Swift's displacement compatibility method. In previous work [4,5] Swift used an empirical relationship to estimate the amount of load transfer present in a fastened doubler. This method has also been shown to be an effective way to estimate load transfer in the layered, finite element code FRANC2D/L [6]. Even though the specimens examined in this study are not of a "doubler-type" configuration explicitly, the symmetry modeling approach used in this study (Figure 2) allows the use of this approach as a reasonable approximation.

The rivet elements in FRANC2D/L are simulated using an elastic spring under shear loading and each portion of the skin and splice plate is an idealized bar element. Bar displacements are obtained using the following equation:

$$\delta_{bar} = \frac{PL}{AE}$$

where:

P = bar load

L = bar length

A = bar area

E = bar modulus

The rivet stiffness was calculated using the following empirical equation:

$$\delta_{riv} = \frac{F \left[A + B \left(\frac{D}{t_D} + \frac{D}{t_s} \right) \right]}{ED}$$

where:

F = applied load (psi)

D = rivet diameter (in)

E = elastic modulus of sheet (psi)

t_d = doubler thickness (in)

t_s = skin thickness (in)

A = 1.666 for steel fasteners

B = 0.86 for steel fasteners

The amount of load transfer present in a given specimen's rivet could then be calculated using the following relationship:

$$\% \text{ Load Transfer} = \frac{\text{Calculated rivet load}}{\text{Applied remote load}} \times 100$$

This approach was used for both the single fastener and multiple fastener, in-line specimen arrangements. These are the only two configurations for which Swift's displacement compatibility method could be applied.

For the multiple fastener, in-line specimen, a "strip" of the joint was modeled in the manner described above. The specimen was also modeled using symmetry conditions through the specimen's thickness. The modeled area of the specimen is shown below in Figure 4.

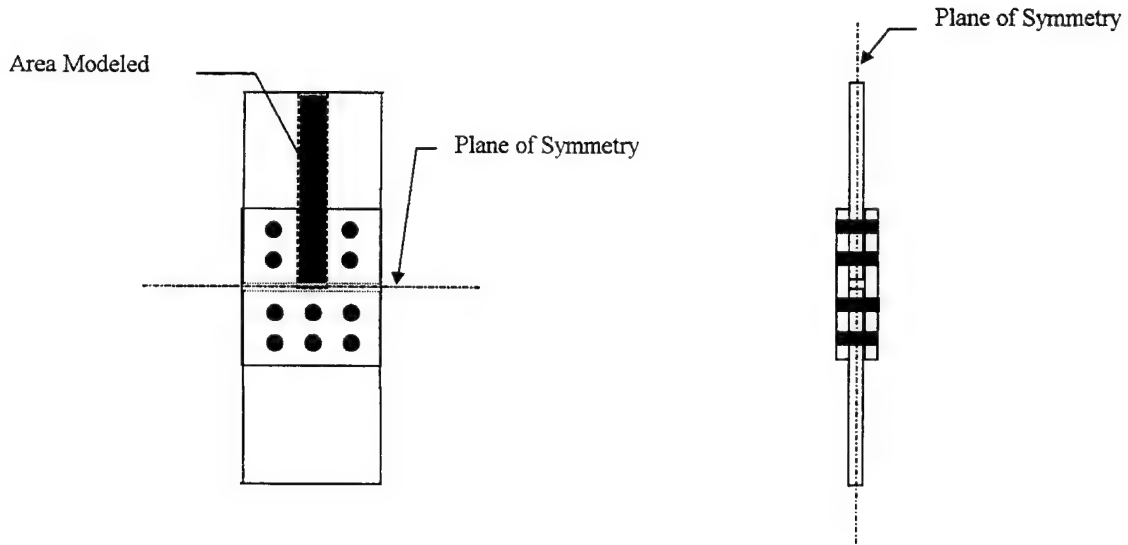


Figure 4: Area Modeled Using FRANC2D/L

A FRANC2D/L finite element analysis was performed to estimate the amount of load transfer present in the critical fastener of the multiple fastener, in-line joint specimen. The FRANC2D/L model is shown below in Figure 5.

The results of the strip model indicated that approximately 53.3% of the load was transferred in the top rivet and 46.7% of the load was transferred from the bottom rivet. Using these values as an approximation, the top three fasteners (including the fastener hole with the crack) were estimated to transfer approximately 17.7 % of the load, while the bottom fasteners were estimated to transfer approximately 15.5% of the load. Even though these numbers would be more representative of an infinitely wide panel (minus edge effects), it is believed that these percentages would be sufficient for providing input for crack growth life predictions of loaded fastener holes.

The multiple fastener, staggered joint specimen arrangement was estimated to have approximately 20% load transfer per fastener (for life predictions), with the fasteners equally sharing the load. This is a rather general approximation, due to the fact that there was no strict control on the finger tight torque between the fasteners and variation in fit between the fasteners, splice plates and joint members. Also, the edge effects in the specimens should have potentially raised the amount of load transferred in the "outer" fasteners of the lower row. This staggered bolt pattern should have eliminated any load interaction or "shadowing" between the two rows of bolts in each joined member. Since Swift's displacement compatibility method has only been shown to be valid for in-line fastener arrangements, it was not employed here. It is believed that this value (20% load transfer) is conservative and should be sufficient for use with "loaded hole" crack growth life prediction analyses of staggered fastener patterned joint specimens.

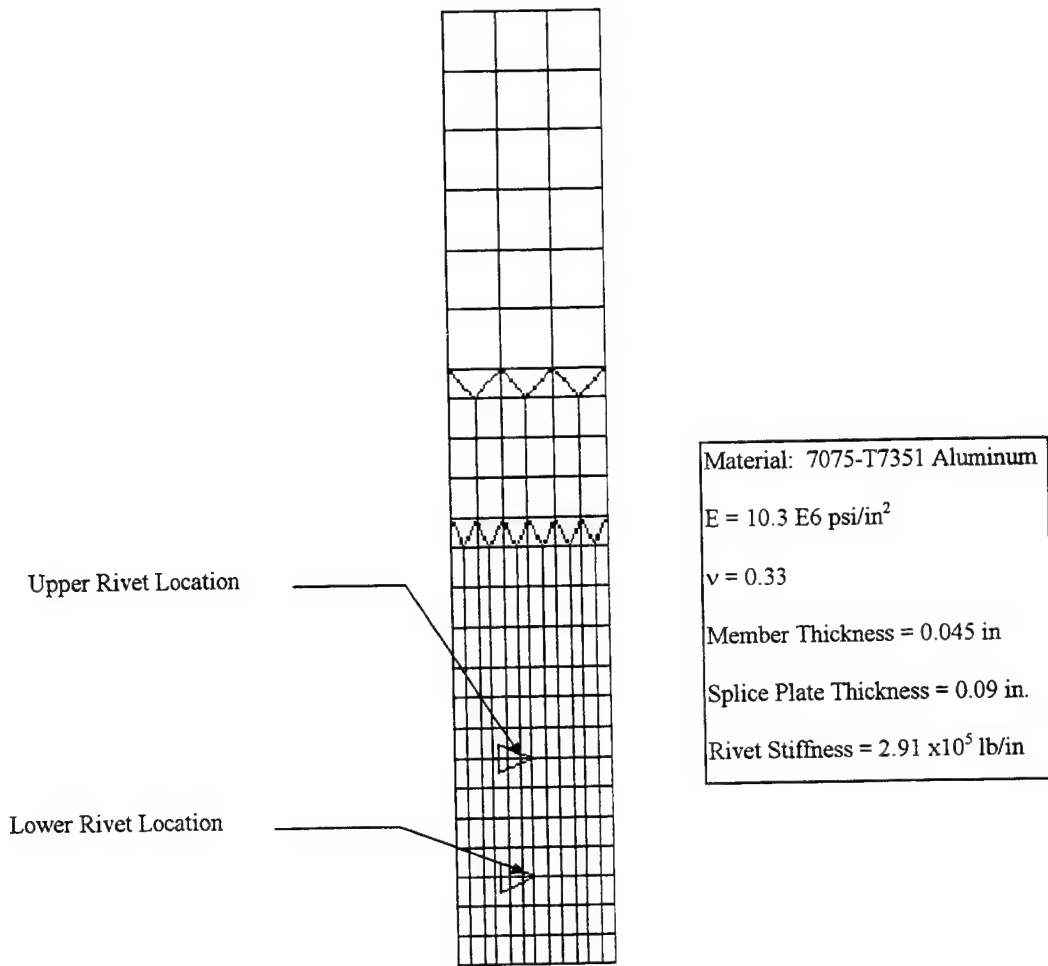


Figure 5: Strip Model of Multi Fastener, In-Line Specimen

4. VERIFICATION TESTING

All verification testing was performed in the Fatigue and Fracture Test Facility, Bldg. 65, Area B, WPAFB, OH. Five servo-hydraulic fatigue test frames were used to test titanium and steel specimens. The test frames were operated in load control with MTS 458 test controllers at frequencies of 6-10 hz. Sinusoidal load control signals were generated with MS-DOS based computers running MATE software.

The test matrix of 40 specimens, listed in Table 1, consisted of center flaw, open hole and joined specimens. All specimens were tested in lab air. A more detailed list including specimen ID, testing dates and machine usage can be found in Appendix A.

Table 1: Test Matrix.

Specimen Type	Max Load (kips)	Stress Ratio (R)	Flawed Specimens	Unflawed Specimens
Center Cracked TI-6AL-4V 0.25 inch thick	decreasing K	-0.1	2	-
		-0.5	2	-
		0.1	2	-
		0.5	2	-
Center Cracked 4340-195ksi Steel 0.25 inch thick	decreasing K	-0.1	2	-
		-0.5	2	-
		0.1	2	-
		0.5	2	-
Corner Cracked Open Hole TI-6AL-4V 0.25 inch thick	16.0	0.1	2	-
	20.0	0.1	2	-
	24.0	0.1	2	-
Single-Fastener Joint 7075-T73	6.0	0.1	3	-
	8.0	0.1	-	3
Multi-Fastener In-Line Joint 7075-T73	8.0	0.1	3	-
	11.0	0.1	-	3
Multi-Fastener Staggered Joint 7075-T73	8.0	0.1	3	-
	11.0	0.1	-	3

4.1. Center Cracked Panel Testing

Titanium (Ti-6-4 AMS 4911G annealed) and 4340-195ksi steel panels (3.95 x 16 x 0.25 inch) with a center through the notch (0.14 X 0.05 inch) tested with a decreasing stress intensity factor method in order to obtain fatigue crack growth rates of 10^{-8} in/cycle. A saw cut extended about 0.02 inch from the end of the notch to facilitate cracking. The specimens were fatigued at a load of 24 kips until cracking began. The load was

decreased at about 7-10% increments and a half crack extension of 0.010" until the crack arrested. The load was then increased at increments of 7-10% until fracture.

4.1.1. Ti-6-4 Center Cracked Panel Testing

Eight titanium specimens (two each at four different R-ratios) were tested. Plots of da/dN versus ΔK for $R=-0.5$, -0.1 , 0.1 , and 0.5 can be seen in Figures 6 – 9, respectively. Note: In all cases where $R<0$, the value ΔK is K_{max} since there is no physical way to define a negative value for K .

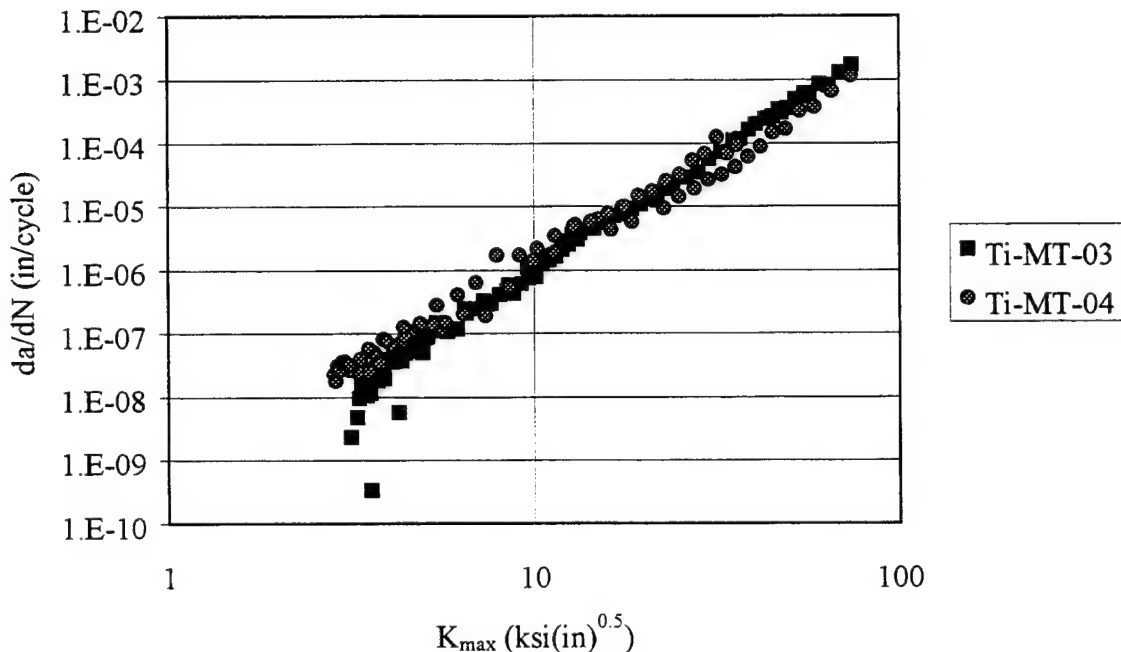


Figure 6: Crack Growth Rate Plot of Ti-6-4 Center Cracked Panels Using the Decreasing K Method with $R=-0.5$.

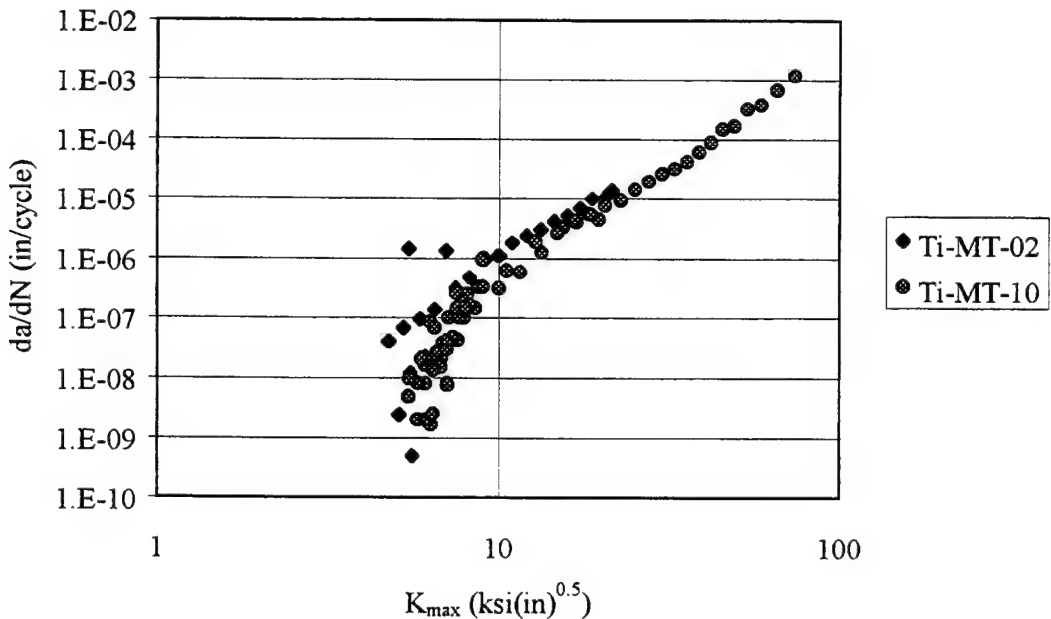


Figure 7: Crack Growth Rate Plot of Ti-6-4 Center Cracked Panels Using the Decreasing K Method with R=-0.1.

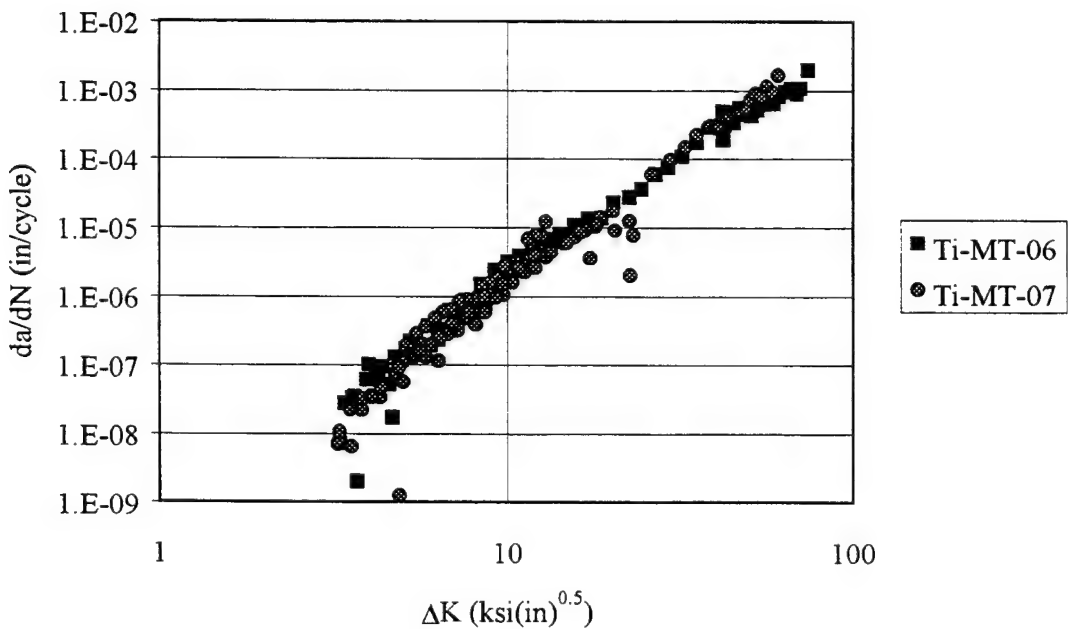


Figure 8: Crack Growth Rate Plot of Ti-6-4 Center Cracked Panels Using the Decreasing K Method with R=0.1.

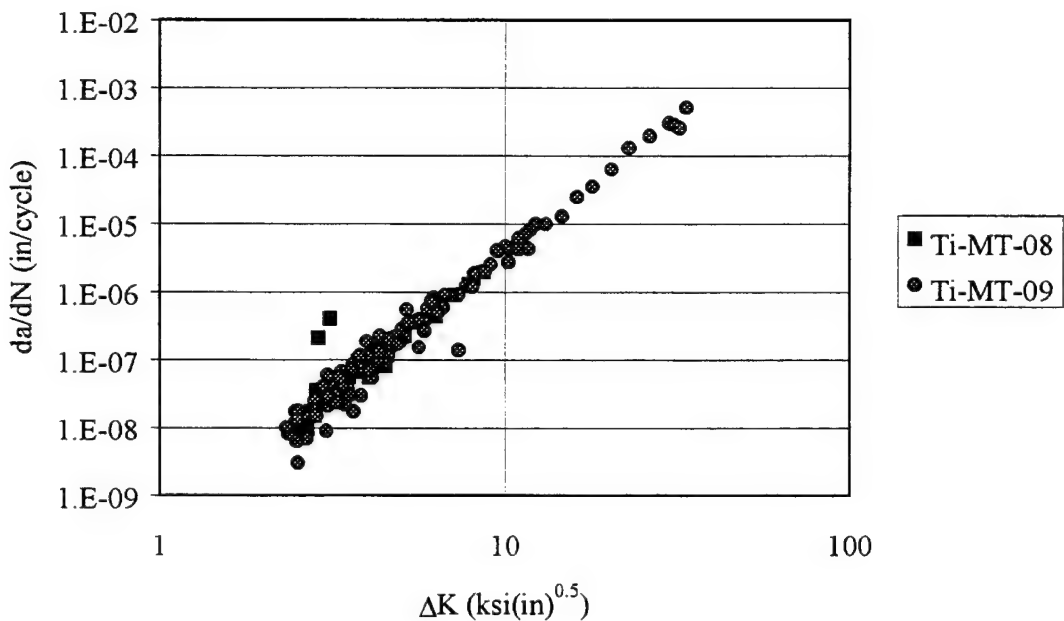


Figure 9: Crack Growth Rate Plot of Ti-6-4 Center Cracked Panels Using the Decreasing K Method with R=0.5.

A composite of all the Ti-6-4 data is shown in Figure 10. Each series of data includes the two specimens represented in Figures 6 - 9. These data were used to modify AFGROW's material data file.

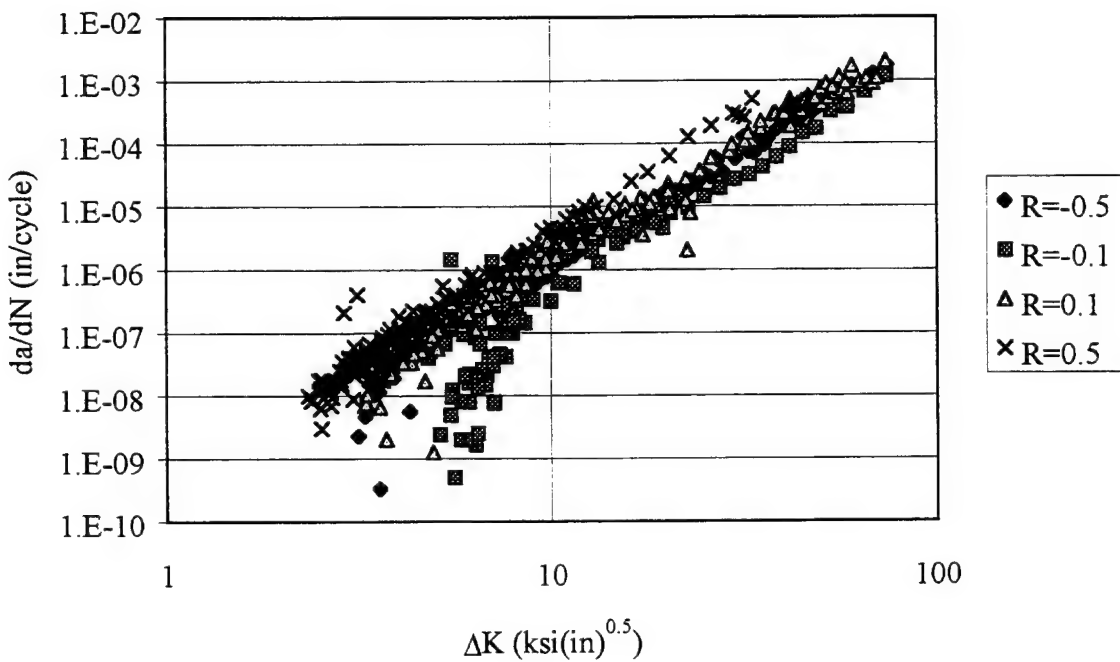


Figure 10: Composite of All Ti-6-4 Center Cracked Panel Tests. Each Series of R-ratio Data Represent Two Specimens.

4.1.2. 4340-195ksi Steel Center Cracked Panel Testing

Eight steel specimens (two each at four different R-ratios) were tested. Plots of da/dN versus ΔK for $R = -0.5, -0.1, 0.1$, and 0.5 can be seen in Figures 11 - 14, respectively. Note: In all cases where $R < 0$, the value ΔK is K_{max} since there is no physical way to define a negative value for K .

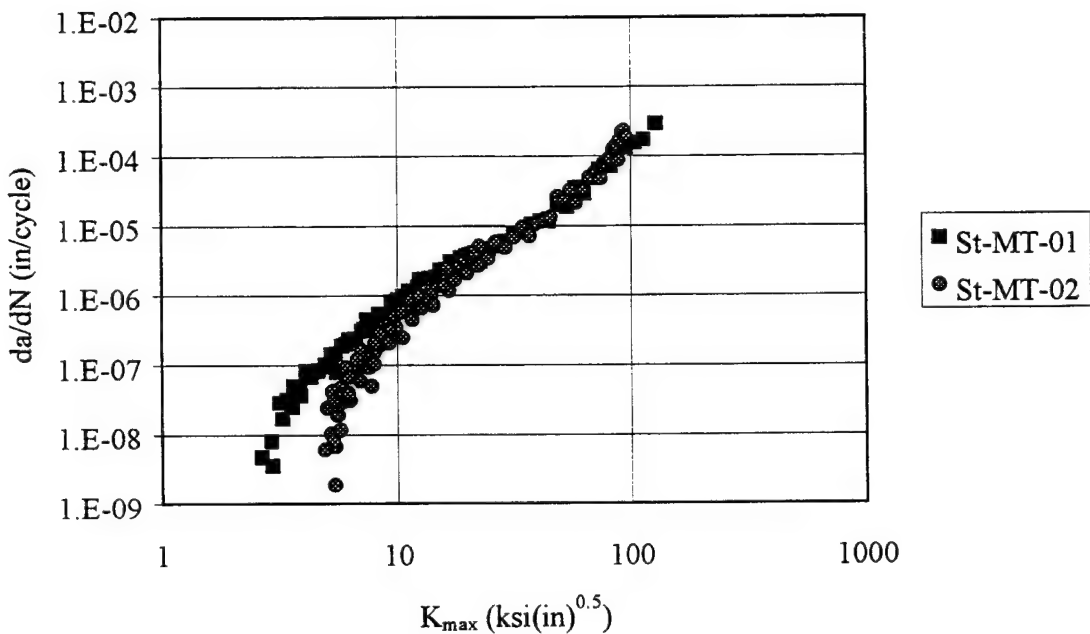


Figure 11: Crack Growth Rate Plot of 4340-195ksi Steel Center Cracked Panels Using the Decreasing K Method with $R=-0.5$.

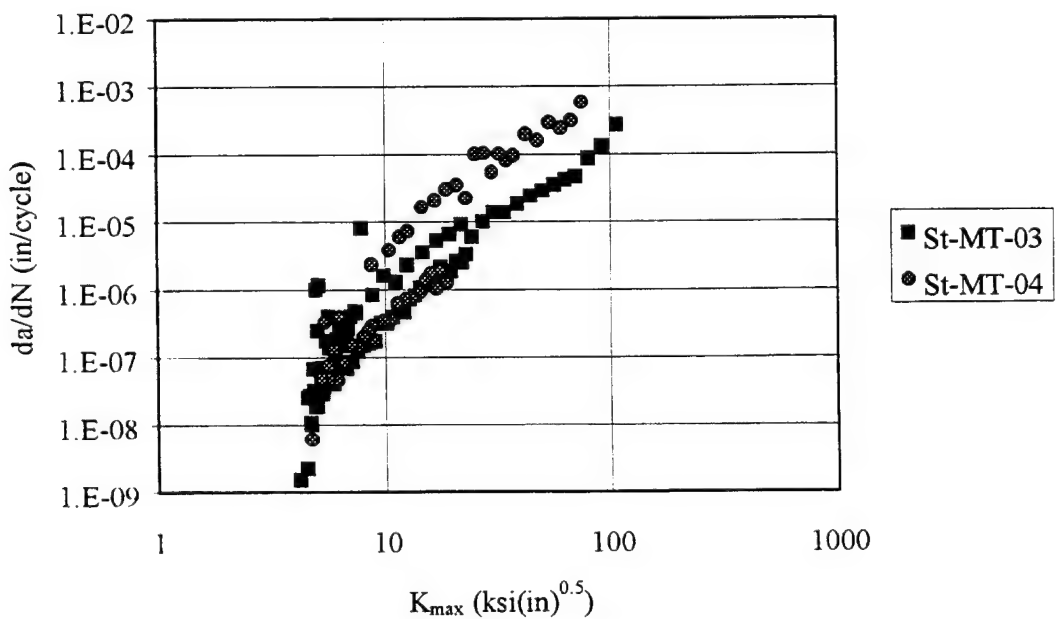


Figure 12: Crack Growth Rate Plot of 4340-195ksi Steel Center Cracked Panels Using the Decreasing K Method with $R=-0.1$.

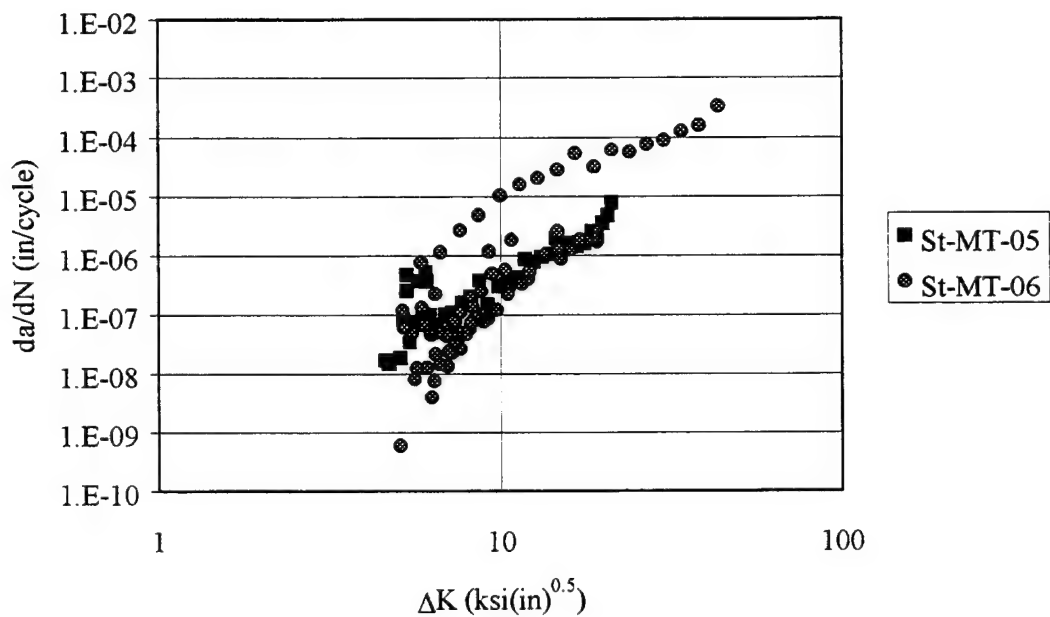


Figure 13: Crack Growth Rate Plot of 4340-195ksi Steel Center Cracked Panels Using the Decreasing K Method with R=0.1.

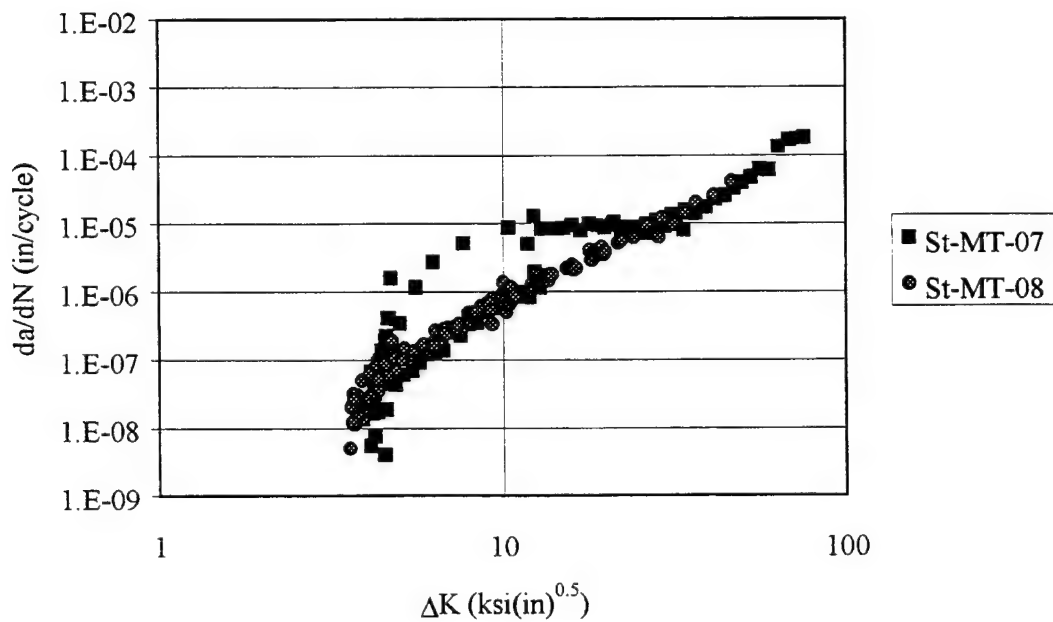


Figure 14: Crack Growth Rate Plot of 4340-195ksi steel Center Cracked Panels Using the Decreasing K Method with R=0.5.

The data for St-MT-07 in Figure 14 are nonlinear because the load was incrementally increased greater than 10% after crack arrest. A composite of all the steel data is shown in Figure 15. Each series of data includes the two specimens represented in Figures 11 - 14. There appears to be two rather distinct curves in Figure 15. The curve which lies in the intersection of $\Delta K=10\text{ksi}\sqrt{\text{in}}$ and $da/dN=1\text{E}-5$ is very atypical of steel data [7]. The data were also compared to test data for 4340-180ksi steel to verify that the test points taken while the load increase was high were unreasonable. These data were removed from the plots and the result is given in Figure 16. These data were used to modify AFGROW's material data file.

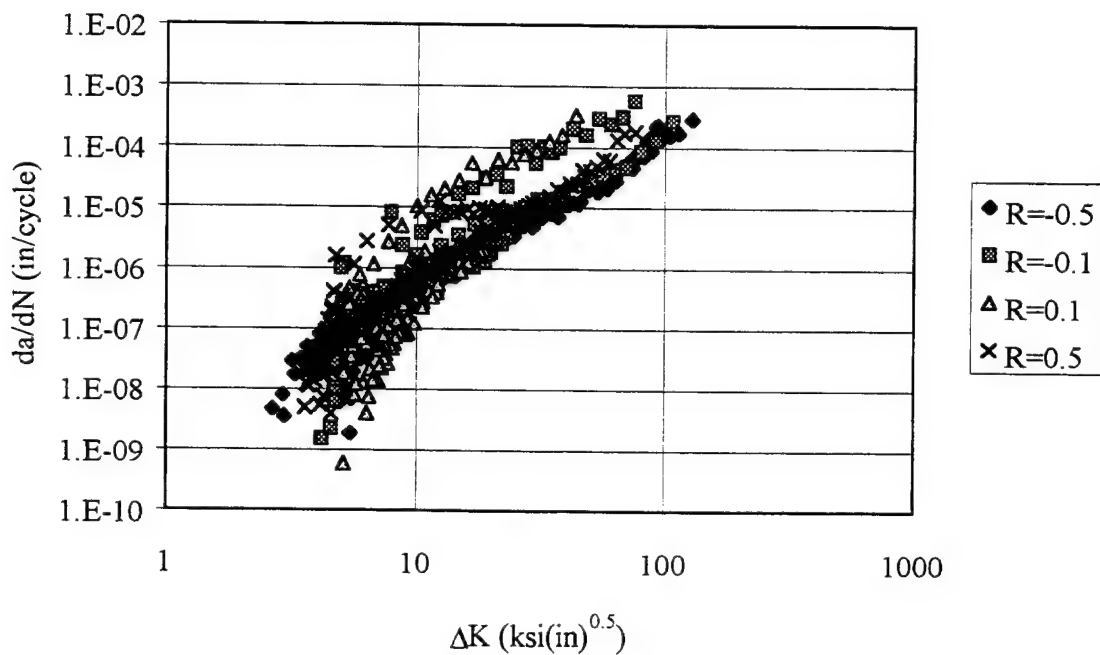


Figure 15: Composite of All 4340-195ksi Steel Center Cracked Panel Tests. Each Series of R-ratio Data Represents Two Specimens.

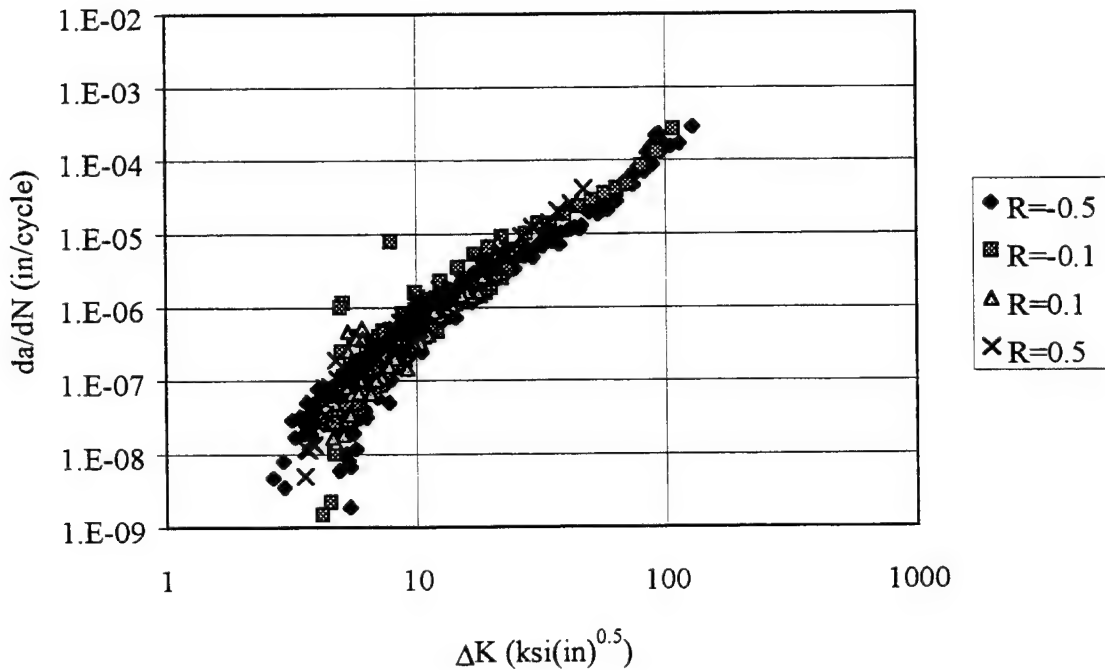


Figure 16: Same Graph as Figure 15 with Unreasonable Data Removed.

4.2. Open Hole Ti-6-4 Panel Testing

Six open hole titanium specimens were tested. A 0.02 to 0.03 inch (length and depth) corner notch was cut on one side of the 0.1875 inch diameter hole. The specimen was precracked at a load of 33 kips until the crack grew 0.06 inch beyond the hole. The hole was then redrilled to 0.25 inch diameter and the specimen was cyclically loaded at the same stress level until the crack length was 0.03 to 0.05 inch beyond the new hole diameter. The specimens were cyclically load shed at 7-10% load increments and 0.1 inch crack increments until the testing load was reached. Two specimens each at loads of 16, 18, and 20 kips, $R=0.1$ were tested. The crack length was recorded at 0.010 inch increments to determine when the corner crack transitioned to a through crack. Once the crack became a through crack the crack length was recorded at 0.1 inch increments until failure.

The crack growth life was compared to AFGROW predictions. AFGROW v3.73 was used with the updated material data file including data generated for this report. The updated material data file was used to make these predictions. A comparison between the test data (from Figure 8) and the fit used in the AFGROW database for Ti-6-4 AMS 4911G annealed is given in Figure 16. Figures 17-22 show the crack growth data for each specimen with the AFGROW prediction. The transition from a corner crack to a through crack is also noted on each graph. The initial crack length was known at the beginning of each test, but the crack depth was not known. The crack depth was estimated using

AFGROW. A 0.025 inch quarter-circle corner crack was grown from a 0.1875 inch hole until crack equaled the original crack length after the hole was redrilled. Due to re-drilling, the aspect ratio of the crack changed. The crack depth was estimated by multiplying the depth of the crack on the 0.1875 inch hole by 0.886 and inputting the result as the crack depth on the 0.25 inch hole. The crack was then grown to emulate the load shedding that occurred before actual test data were taken. The initial crack sizes input to AFGROW are located in Table 2. AFGROW was then restarted and the results are plotted in Figures 17 - 22 along with the data for each specimen. In some cases, a second crack formed on the opposite side of the hole during a test. The effect of this cannot currently be predicted using AFGROW. However, it will cause acceleration in growth of the primary crack.

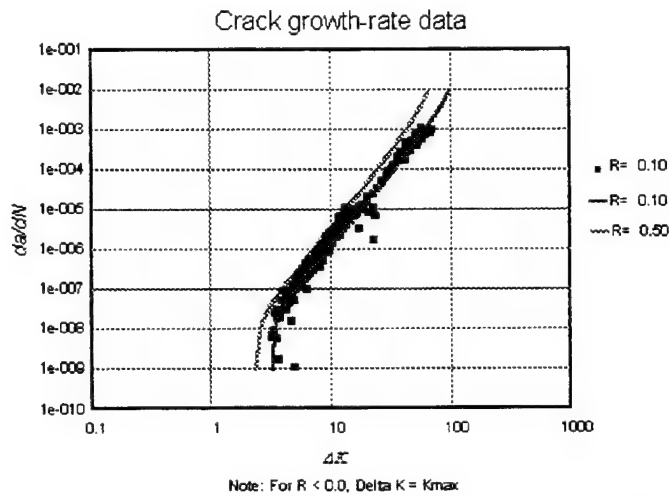


Figure 17: Test Data Shown in Figure 8 Plotted with AFGROW Database Plot for Various R-ratios.

Table 2: Crack Sizes Input to AFGROW for Life Prediction Shown in Figures 17 - 22.

Specimen	Crack length, c	Crack depth, a
Ti-OH-01	0.087	0.128
Ti-OH-02	0.103	0.146
Ti-OH-03	0.047	0.080
Ti-OH-04	0.049	0.082
Ti-OH-05	0.055	0.094
Ti-OH-06	0.081	0.119

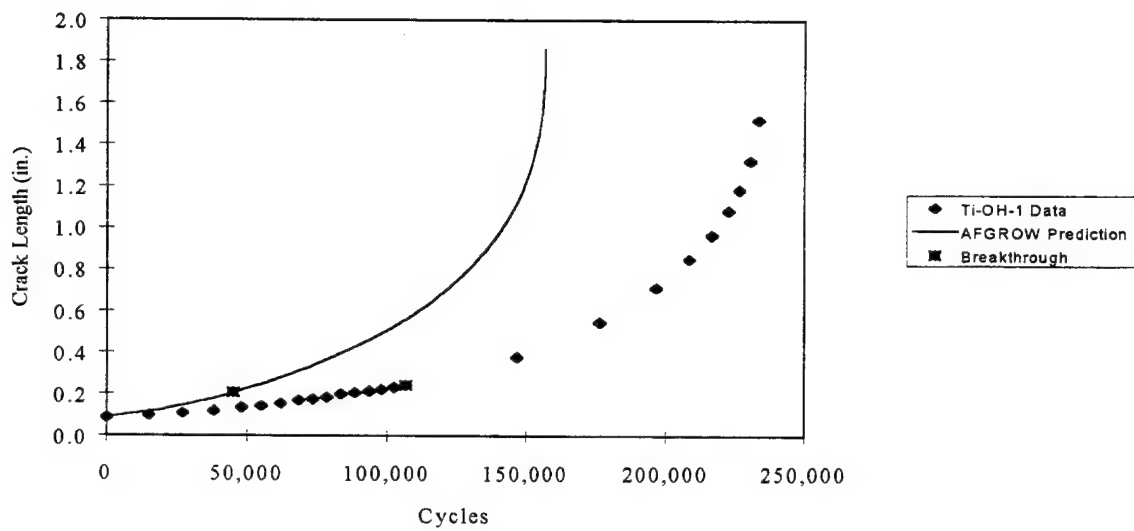


Figure 18: Constant Amplitude (16 kips) Testing Data of Ti-OH-1 and AFGROW Prediction.

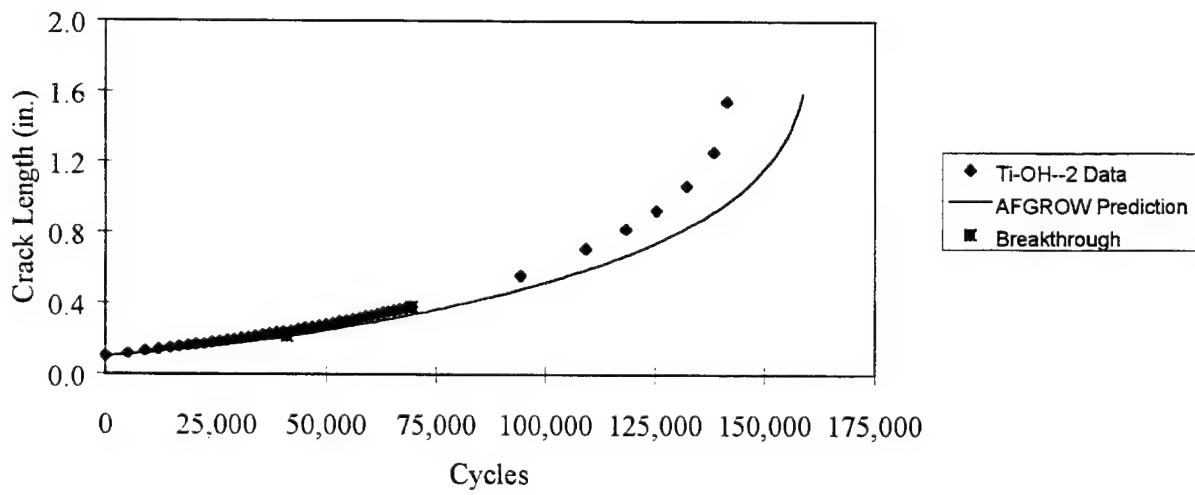


Figure 19: Constant Amplitude (16 kips) Testing Data of Ti-OH-2 and AFGROW Prediction.

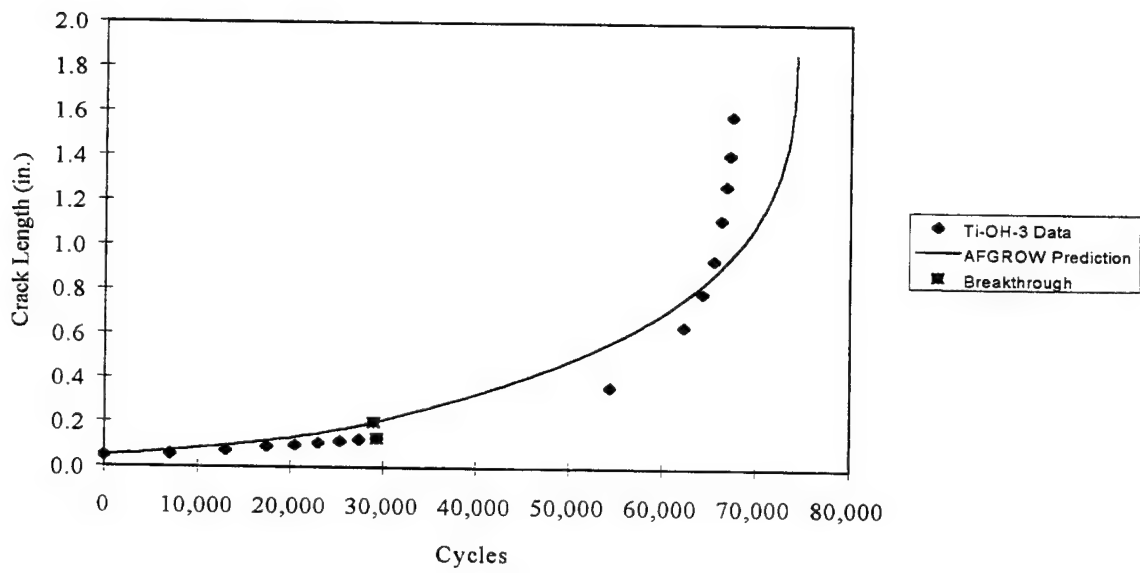


Figure 20: Constant Amplitude (18 kips) Testing Data of Ti-OH-3 and AFGROW Prediction.

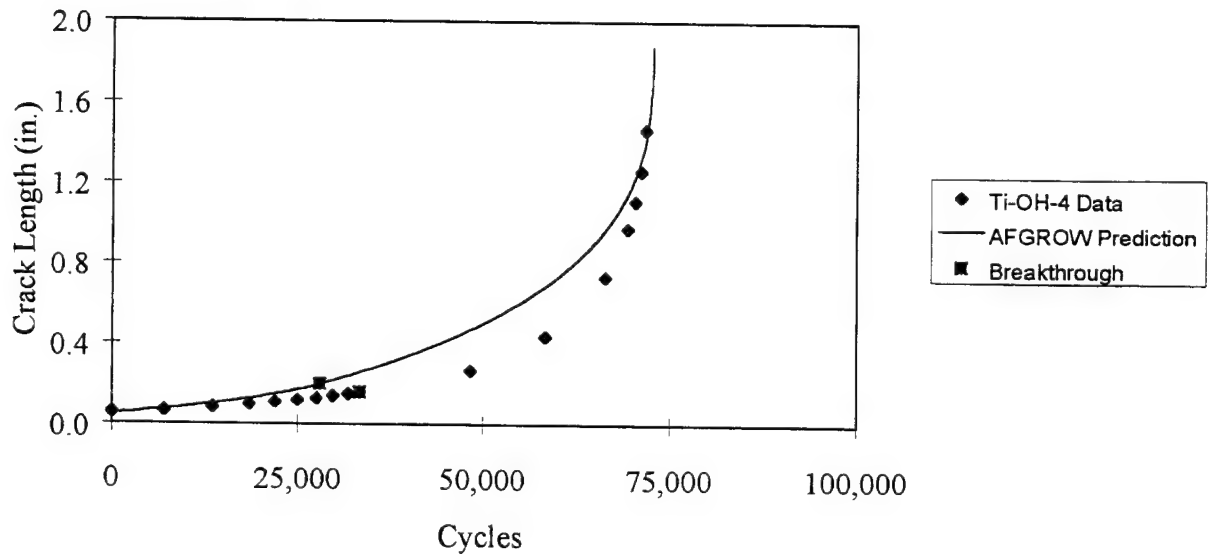


Figure 21: Constant Amplitude (18kips) Testing Data of Ti-OH-4 and AFGROW Prediction.

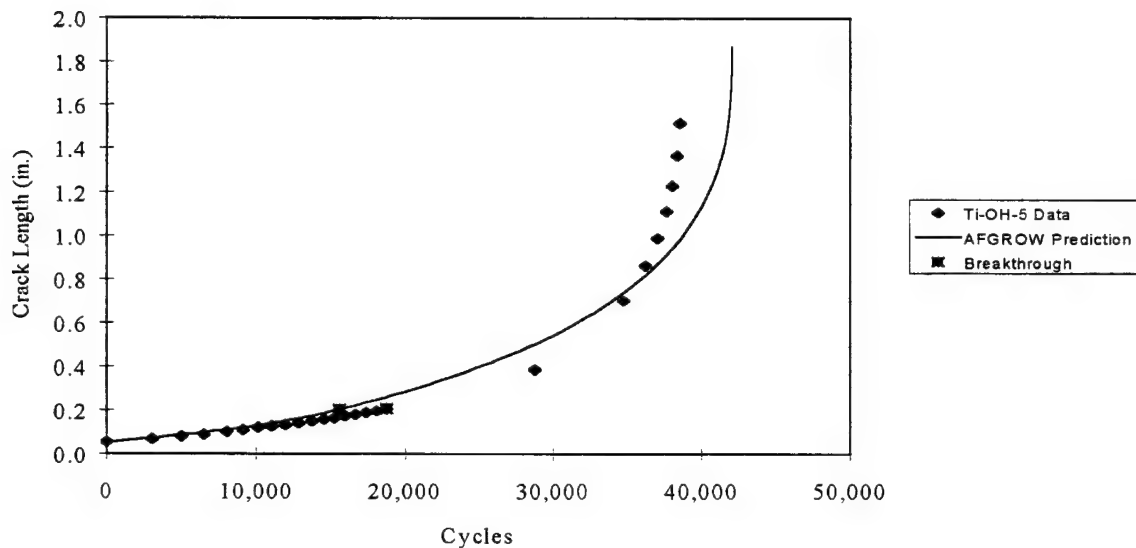


Figure 22: Constant Amplitude (20 kips) Testing Data of Ti-OH-5 and AFGROW Prediction.

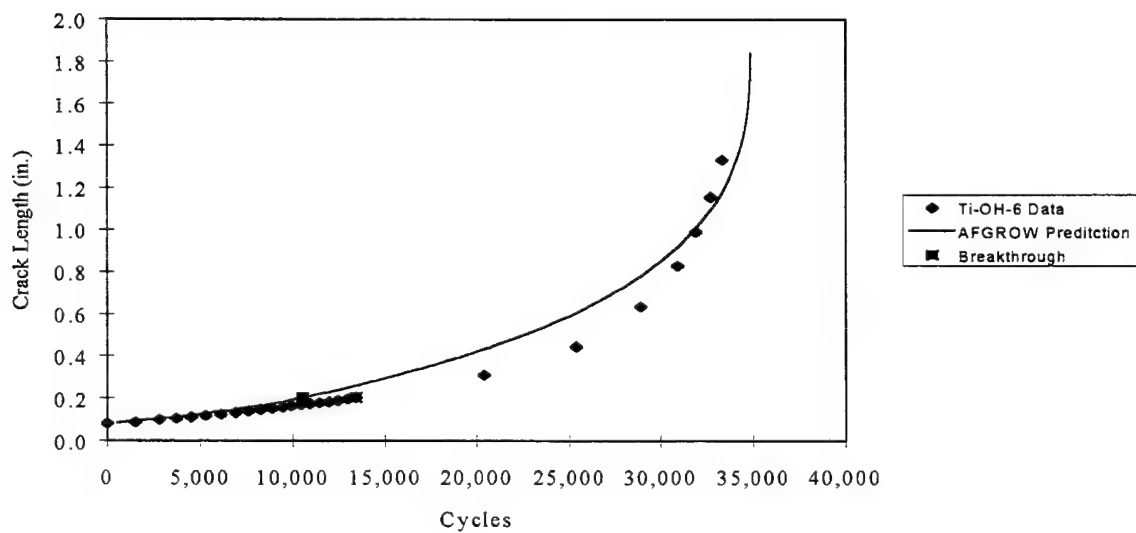


Figure 23: Constant Amplitude (20 kips) Testing Data of Ti-OH-6 and AFGROW Prediction.

4.3. Fastener Joint Specimens

Flawed and unflawed fastener joint specimens, seen in Figure 1, were fatigue tested under constant amplitude conditions until failure. The flawed specimens were precracked in the same manner as the open-hole titanium specimens. The panels with a single 0.1875 inch open hole and an initial corner saw cut of 0.02-0.03 inch length and depth were precracked to a length of 0.07 inch. The panels were then cut in half to a length of 8 inches and the precracked hole was then redrilled to 0.25 inch diameter (leaving a 0.04 inch precrack). A schematic of a specimen is shown in Figure 23. The panels were then riveted together as shown in Figure 1. The cracked hole was in the top middle hole of the in-line joint specimen and in one of the top holes with the crack growing towards the other rivet in the staggered joint specimen. The test matrix and lifetimes are shown in Appendix.

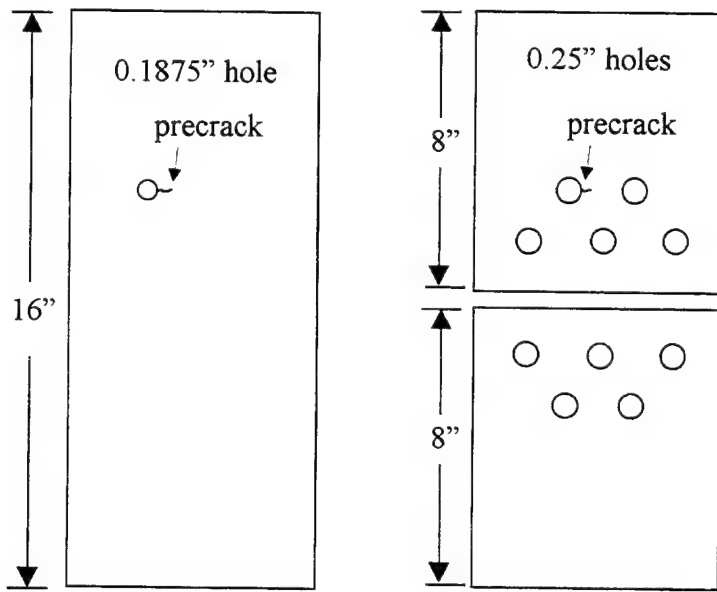


Figure 24: Schematic of the Joint Specimens After Precracking but Before Riveting.

4.4. AFGROW Predictions of Joint Specimens

Using initial conditions, AFGROW was used to predict the lifetimes of the specimens. The test results were compared to AFGROW predictions. The AFGROW predictions were handled in the same manner as the open hole specimens. An initial saw cut was modeled as a quarter circle corner crack in a 0.1875 inch diameter hole. The crack was then grown to the known length before the hole was drilled to 0.25 inch. Then the test prediction began. In order to predict the life of a joint specimen with AFGROW, the specimen

configuration must first be modeled. The single joint configuration was easy to model with AFGROW. The corner crack at open hole configuration was chosen with a load transfer of 100%. (100% of the load was introduced through the fastener.)

Modeling the load transfer coefficient for the staggered and in-line joint specimens is more complicated however. To further illustrate the load transfer, consider Figure 24. The stresses at the edge of the holes at cut A result from bearing stresses from the loaded fasteners in cut A as well as bypass stresses from the loaded fasteners in cut B. The stress at the edge of the holes at cut B, however, is a result of bearing stresses only from the loaded fasteners in cut B. The equation for determining the load transfer coefficient is given by:

$$L.T_A = \frac{2P_a}{3P_b + 2P_a} \quad \text{or} \quad L.T_B = \frac{3P_b}{3P_b}$$

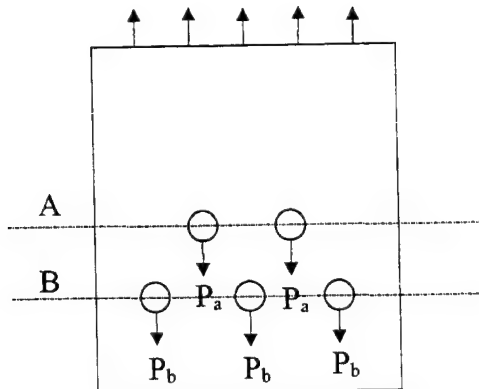


Figure 25: Schematic of Staggered Joint Specimen and Loads Used to Calculate Load Transfer Coefficient.

The load transfer per fastener was discussed in Section 1, and for the staggered joint specimens, the load transfer per fastener was determined to be 20%. Since only two of the five rivets of the staggered joint specimens are in the top, the load transfer coefficient is 40%. The staggered joint specimens were modeled as an open hole with a double corner crack. Although only one of the holes was precracked, examination of the fracture surface showed that a crack appeared to grow from the other hole at an equal rate and coalesced, and the two cracks coalesced midway between the holes. For this reason the specimen was assumed to be fractured when the crack length was 0.375inch. The width of the specimens was assumed to be 1.75 inch since that is half the distance to the nearest hole. Although the width of the specimen was 3.95 inches, a width of 1.75 inches was used because the nearest hole was assumed to be an edge. This engineering approximation is reasonable because as the crack approaches the hole, it will speed up as if it is approaching an edge, and once the crack reaches the adjacent hole, the rest of the life is short compared to the time it took to reach the hole.

For the in-line joint specimens, the specimens were modeled as a single hole with a corner crack. The top row of in-line rivets shadow the bottom row, which results in the top row transferring 53.3% of the load, as discussed in the finite element section. The adjacent hole was 0.875 inch from the cracked hole, and the width of the modeled specimens was twice that distance, 1.75 inches.

The predicted fatigue lives are compared to the actual lifetimes and the results are shown in Table 3. The single, in-line, and staggered joint specimens had an average error of 18%, 4%, and 19%. These results are promising considering that AFGROW currently does not have the capability to model multiple hole specimens.

**Table 3: Flawed Riveted Specimen Lifetimes and Information Used for AFGROW Predictions
Where c is Measured and a is Calculated.**

Specimen	Type	Stress (ksi)	c (in.)	a (in.)	Lifetime	Prediction
4-04	single	6	0.036	0.0779	416,632	274,073
4-05	single	6	0.039	0.0814	302,224	268,155
4-06	single	6	0.048	0.0918	236,673	256,000
5A-07	in-line	8	0.040	0.0693	151,008	146,461
5A-08	in-line	8	0.039	0.0684	139,660	146,725
5B-07	staggered	8	0.039	0.0684	54,945	75,000
5B-08	staggered	8	0.042	0.0710	73,540	74,000

5. AFGROW ENHANCEMENTS

Various features, including residual stress effects, multi-dimensional crack growth rate data, user input beta factor table, and real-time plotting have been added to AFGROW.

The multi-dimensional crack growth rate data have been added to predict the crack growth life of a structure which may experience a variety of environments during its lifetime. Crack growth rate data can be stored and retrieved for a given material under different environmental conditions. The data can be accessed according to their environmental condition as a function of crack position. The enhancement has the following specifics: 1) user can input modified crack growth rated data for a given material under different environmental conditions, 2) user can save crack growth data to a file or read crack growth data from a file, 3) user-input crack growth rate data can be used with both tabular material data and Walker equation options, 4) user can specify environmental condition and region around a crack as a function of distance "c" (surface direction) and "a" (thickness direction, where applicable) ahead of the crack front(s), 5) AFGROW will transition from one environmental condition to another by a polynomial function (to third order), as the crack grows. The environment dialog box and specimen model with two environments can be seen in Figures 25 and 26, respectively.

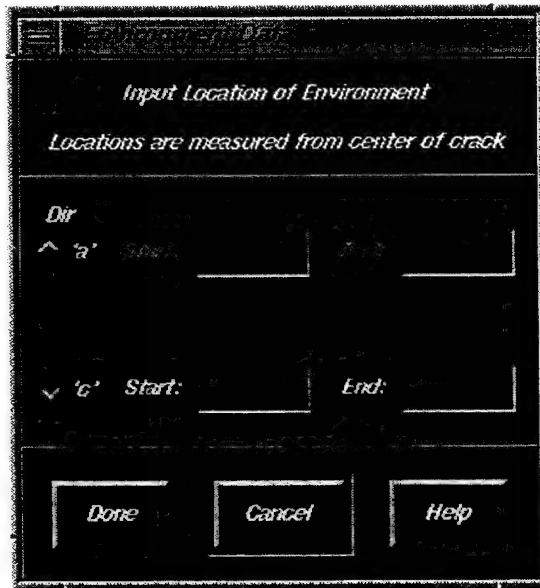
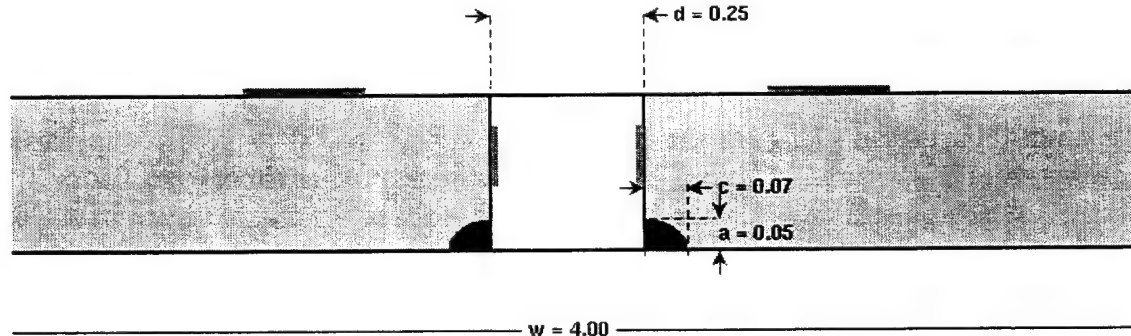


Figure 26: Environment Dialog Box.

Double corner crack at hole



Environments:

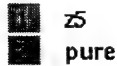


Figure 27: Model With Two Environments Applied.

The Beta correction table allows the user to enhance the standard solutions currently used to calculate the crack driving parameter, K . For example, consider a crack emanating from a notch with a large stress concentration. First to model this situation, a standard crack configuration is chosen, then the Beta correction table is used to modify the crack driving force as a function of distance from the notch. More specifically, the input Beta Factor table will operate as such: 1) AFGROW default will have the Beta Factor modification turned off, 2) the user input Beta Factor table could be input manually, or read from a file, 3) the user-input Beta Factor table function can be turned off/on at any time. In addition, the graphical user interface will be written so that the appropriate portions of the code will be disabled when the capability is used, and that existing methods remain in the code after this modification is made. The Beta Factors dialog box can be seen in Figure 27.

BETA FACTORS

Input Normalized Stress Distributions
in the following format

Use up to 25 sets of values for increasing 'z' distances

At z = 0, Stress(x) and Stress(y) have been set to 1.0
Subsequent values are normalized wrt Stress at z = 0

Set	Z Coord	Stress(X)	Stress(Y)
0	0.0	1.0	1.0
1	1.0	1.0	1.0
2	2.0	1.0	1.0
3	3.0	1.0	1.0
4	4.0	1.0	1.0
5	5.0	1.0	1.0
6	6.0	1.0	1.0
7	7.0	1.0	1.0
8	8.0	1.0	1.0
9	9.0	1.0	1.0
10	10.0	1.0	1.0
11	11.0	1.0	1.0
12	12.0	1.0	1.0
13	13.0	1.0	1.0
14	14.0	1.0	1.0
15	15.0	1.0	1.0
16	16.0	1.0	1.0
17	17.0	1.0	1.0
18	18.0	1.0	1.0
19	19.0	1.0	1.0
20	20.0	1.0	1.0
21	21.0	1.0	1.0
22	22.0	1.0	1.0
23	23.0	1.0	1.0
24	24.0	1.0	1.0
25	25.0	1.0	1.0

Done **Cancel** **Help**

Figure 28: Beta Factor Table.

Real time plotting and output file creation have been added to AFGROW. The real time plotting capability plots the crack length versus cycles while AFGROW is running. Up to eight different conditions can be overlaid on the same plot. The output file contains data columns of crack length, cycles, stress intensity, beta, stress ratio, stress, and crack growth rate. The plot window can be seen in Figure 28.

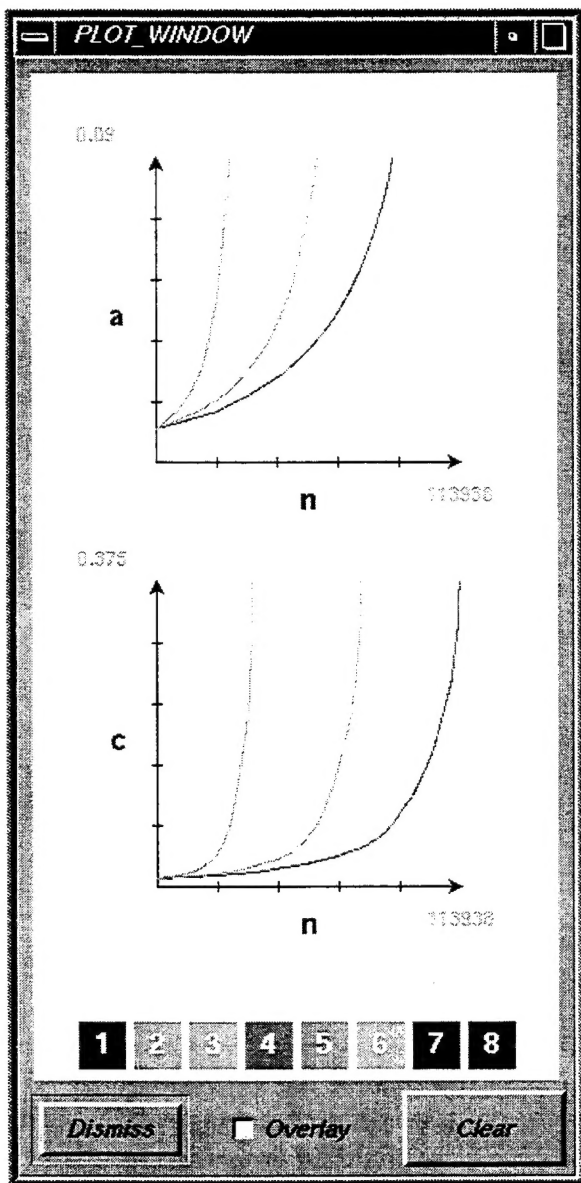


Figure 29: Plot Window Showing Crack Length Versus Cycles.

6. REFERENCES

- [1] Boyd, K.L., Jansen, D.A., Krishnan, S., Harter, J.A., " Structural Analysis and Verification of Aircraft Structures, Vol. I. Characterization of 7075-T7351 Aluminum; MODGRO Verification; MODGRO GUI Development," *WL-TR-95-3090*, Air Force Flight Dynamics Directorate, Wright-Patterson Air Force Base, OH, January 1996.
- [2] Krishnan, S., Boyd, K.L., Harter, J.A., "AFGROW User's Manual: Version 3.0.4," *WL-TM-96-3096*, Air Force Flight Dynamics Directorate, Wright-Patterson Air Force Base, OH, July 1995.
- [3] Wawrynek, P. and Ingraffea, A.R., "Interactive Finite Element Analysis of Fracture Processes: An Integrated Approach," *Theoretical and Applied Fracture Mechanics*, Vol. 8, 1987, pp. 137-150.
- [4] Swift, T., "Damage Tolerance Analysis of Redundant Structures," *Fracture Mechanics Design Methodology, AGARD-LS-97*, North Atlantic Treaty Organization, London, England, Jan. 1979, pp 5-1 - 5-33.
- [5] Swift, T., "Repairs to Damage Tolerant Aircraft." *Structural Integrity of Aging Airplanes*, Springer Verlag, 1991, pp. 433-484.
- [6] Gondhalekar, S., "Development of a Software Tool for Crack Propagation Analysis in Two Dimensional Layered Structures," *Master's Thesis*, Department of Mechanical Engineering, Kansas State University, Manhattan, KS, 1992.
- [7] Skinn, D.A., Gallagher, J.P., Berens, A.P., Huber, P.D. Smith, J., *Damage Tolerant Design Handbook*, University of Dayton Research Institute, Dayton, OH, 1994, pp. 3-176.

7. APPENDIX

7.1 Detailed Specimen Information

Flawed Center Cracked Titanium - Decreasing K Testing (da/dn = 1.0e-8)							
Spec ID #	Mach	W	t	oad (kips)	R	Begin	End
Ti-MT-02	13	3.9505	0.26040	24.9	-0.1	07-19-95	Overload
Ti-MT-03	12	3.9505	0.25820	24	-0.5	11/3/95	4/9/96
Ti-MT-04	4	3.9500	0.25240	24	-0.5	11-15-95	3/27/96
Ti-MT-06	12	3.9500	0.26480	26	0.1	07-24-95	11-03-95
Ti-MT-07	13	3.9500	0.25910	24	0.1	10-25-95	3/26/96
Ti-MT-08	10	3.9500	0.25680	24	0.5	11-20-95	4/12/96
Ti-MT-09	1	3.9500	0.25710	24	0.5	11-15-95	6/13/96
Ti-MT-10	13	3.9500	0.25900	24	-0.1	3/27/96	5/17/96

Flawed Center Cracked Steel - Decreasing K testing							
Spec ID #	Mach	W	t	oad (kips)	R	Begin	End
St-MT-01	10	3.945	0.213	30	-0.5	4/24/96	5/24/96 cf not straight
St-MT-02	10	3.95	0.212	30	-0.5	5/30/96	7/16/96
St-MT-03	12	3.9485	0.211	30	-0.1	4/25/96	6/11/96
St-MT-04	12	3.94	0.225	30	-0.1	6/12/96	7/2/96
St-MT-05	4	3.9465	0.214	30	0.1	5/2/96	5/30/96 not grow-grow
St-MT-06	4	3.95	0.226	30	0.1	5/30/96	8/5/96
St-MT-07	13	3.95	0.208	30	0.5	6/7/96	7/25/96
St-MT-08	12	3.952	0.235	30	0.5	7/2/96	8/20/96

Flawed Open Hole Titanium - Constant Load Testing								
Spec ID #	Mach	W	t	oad (kips)	R	Cycles	Begin	End
Ti-OH-01	4	3.956	0.251	16	0.1	233,650	4/17/96	4/19/96
Ti-OH-02	4	3.946	0.257	16	0.1	141,226	4/22/96	4/23/96
Ti-OH-03	10	3.9615	0.24	20	0.1	67,450	4/18/96	4/18/96
Ti-OH-04	10	3.9465	0.24	20	0.1	71,750	4/19/96	4/19/96
Ti-OH-05	10	3.947	0.249	24	0.1	38,577	4/22/96	4/22/96
Ti-OH-06	10	3.949	0.245	24	0.1	33,320	4/23/96	4/23/96

Flawed Single Fastener Joint						
Spec ID #	Mach	W	t	PreCrack	Stress (ksi)	Cycles
4-04	13	1.0055	0.250	0.036	6.0	416,632
4-05	13	1.0050	0.250	0.039	6.0	302,224 approx (Power Out)
4-06	13	1.0050	0.250	0.048	6.0	236,673

Unflawed Single Fastener Joint						
Spec ID #	Mach	W	t	PreCrack	Stress (ksi)	Cycles
4-01	12	1.0049	0.250	--	8.0	400,211
4-02	12	1.0050	0.250	--	8.0	244,675
4-03	12	1.0050	0.250	--	8.0	235,616 approx (Power Out)

Flawed Multi Fastener In Line Joint						
Spec ID #	Mach	W	t	PreCrack	Stress (ksi)	Cycles
5A-07	12	3.9380	0.090	0.040	8.0	151,008 After Bolts Loosened (52,253)
5A-08	12	3.9380	0.090	0.039	8.0	139,660 Bolts Loose

Unflawed Multi Fastener In Line Joint						
Spec ID #	Mach	W	t	PreCrack	Stress (ksi)	Cycles
5A-01	12	3.9500	0.090	--	11.0	524,611 Bolts Tight
5A-02	12	3.9485	0.090	--	11.0	98,793 Bolts Loose
5A-03	12	3.9480	0.090	--	11.0	77,676 After Bolts Loosened (223,627)

Flawed Multi Fastener Staggered Joint						
Spec ID #	Mach	W	t	PreCrack	Stress (ksi)	Cycles
SB-07	13	3.9390	0.090	0.039	8.0	57,945 After Bolts Loosened (52,060)
SB-08	13	3.9350	0.090	0.042	8.0	73,540 Bolts Loose

Unflawed Multi Fastener Staggered Joint						
Spec ID #	Mach	W	t	PreCrack	Stress (ksi)	Cycles
SB-01		3.9490	0.090	--	11.0	45,922 Bolts Loose
SB-02		3.9490	0.090	--	11.0	54,327 Bolts Loose
SB-03		3.9490	0.090	--	11.0	58,115 Bolts Loose